Coherent diffraction of hydrogen through the 246 pm lattice of graphene

Christian Brand, Maxime Debiossac, Toma Susi, François Aguillon, Jani Kotakoski, Philippe Roncin, Markus Arndt

PAPER • OPEN ACCESS

Coherent diffraction of hydrogen through the 246 pm lattice of graphene

New Journal of Physics
The open access journal at the forefront of physics

Deutsche Physikalische Gesellschaft DPG
IOP Institute of Physics

Published in partnership with: Deutsche Physikalische Gesellschaft and the Institute of Physics

OPEN ACCESS

RECEIVED
6 November 2018

REVISED
24 December 2018

ACCEPTED FOR PUBLICATION
11 February 2019

PUBLISHED
15 March 2019

PAPER

Coherent diffraction of hydrogen through the 246 pm lattice of graphene

Christian Brand[1], **Maxime Debiossac**[1], **Toma Susi**[1], **François Aguillon**[2], **Jani Kotakoski**[1], **Philippe Roncin**[2] and **Markus Arndt**[1]

[1] University of Vienna, Faculty of Physics, PNM, Boltzmanngasse 5, A-1090 Vienna, Austria
[2] Institut des Sciences Moléculaires d'Orsay (ISMO), CNRS, Univ. Paris-Sud, Université Paris-Saclay, F-91405 Orsay, France

E-mail: brandc6@univie.ac.at

Keywords: matter-wave diffraction, 2D materials, density functional theory, atomic interference

Supplementary material for this article is available online

Abstract

We study the diffraction of neutral hydrogen atoms through suspended single-layer graphene using molecular dynamics simulations based on density functional theory. Although the atoms have to overcome a transmission barrier, we find that the de Broglie wave function for H at 80 eV has a high probability to be coherently transmitted through about 18% of the graphene area, contrary to the case of He. We propose an experiment to realize the diffraction of atoms at the natural hexagon lattice period of 246 pm, leading to a more than 400-fold increase in beam separation of the coherently split atomic wave function compared to diffraction experiments at state-of-the art nano-machined masks. We expect this unusual wide coherent beam splitting to give rise to novel applications in atom interferometry.

1. Introduction

De Broglie's seminal hypothesis on the wave-particle duality of massive matter [1] has been corroborated by numerous famous experiments, starting with pioneering studies using electrons [2, 3], neutrons [4], helium [5], and atomic [6] and molecular hydrogen [5] diffracted at single crystals. Interestingly, diffraction in transmission through crystalline structures has not yet been demonstrated for objects more complex than electrons and neutrons. Even the thinnest conceivable material, a single layer of graphene, constitutes an impermeable membrane for thermal atomic beams including helium [7–9]. However, implantation experiments have shown that helium with a suitable kinetic energy can be captured inside the fullerene ion C_{60}^{+} without inducing molecular fragmentation [10]. This raises the question whether it is also possible to diffract fast atoms through graphene. A key requirement for such an experiment is that the incident particle behaves like a delocalized wave and that its transverse coherence encompasses several grating slits. However, one might wonder whether interactions between the matter-wave and the grating might reveal which path the atom took. This (partial) decoherence of the matter-wave could eventually lead to the localization of the atom to a single hexagon of the graphene membrane. In this case, coherent diffraction would be no longer possible.

Here, we investigate the diffraction of a fast atomic hydrogen beam through a single-layer graphene membrane using both wave packet propagation (WPP) and the semi-classical eikonal approximation. The penetration of neutral H atoms through the center of a carbon hexagon of a graphene monolayer is simulated using time-dependent density functional theory molecular dynamics (TDDFT/MD). Although sizable electronic excitation is predicted, the results indicate that coherent diffraction through single-layer graphene is feasible, leading to widely separated coherent beams of atomic hydrogen.

To the best of our knowledge, this is the first study discussing atomic diffraction through crystalline materials. Single-layer graphene was chosen as it is the most robust free-standing 2D membrane available, both electronically and mechanically. Furthermore, it has the smallest lattice spacing and represents thus the ultimate grating in this respect. Diffraction through such a material is very important both from a theoretical and

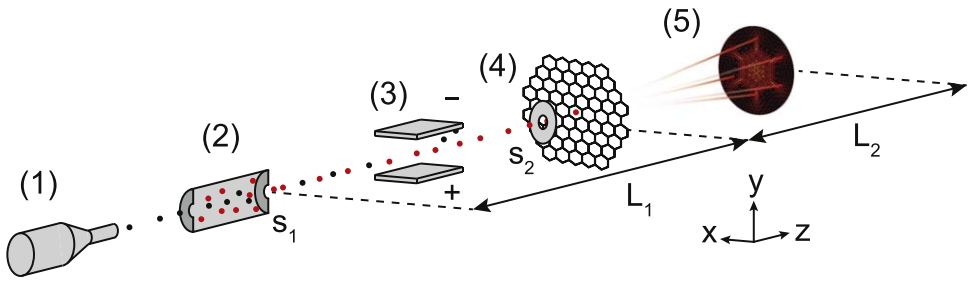

Figure 1. Schematic of the proposed experiment. Fast atomic hydrogen ions (black) are produced in a commercial ion gun (1) and neutralized in an effusive cell (2) by resonant charge transfer. Remaining ions are removed by a static electric field (3). After propagating the distance L_1 the beam is collimated by an aperture with a diameter s_2. Directly behind the collimator the atoms are diffracted at single-layer graphene (4) according to their de Broglie wavelength λ_{dB}. The diffraction pattern is recorded at a distance L_2 by a micro-channel plate amplifier (5) stacked onto a phosphor screen and a CCD camera. Here we consider $L_1 = L_2 = 1$ m and $s_1 = s_2 = 200$ μm.

experimental point of view. On the one hand, interference is possible even though the matter-wave loses a significant amount of energy to the diffracting structure. As a result, the different couplings to the membrane will leave their traces in the diffraction pattern, bringing energy-resolved interaction studies of the matter-wave with 2D materials within reach. On the other hand, the transverse coherence of the atoms stretches over meters on reasonable length scales, opening new vistas for various matter-wave interference experiments.

2. Transmission of hydrogen through graphene

To simulate the transmission of H through a perfect graphene monolayer we use TDDFT/MD [11–15] (i.e. Ehrenfest dynamics [16]) as implemented in the projector-augmented-wave (PAW) based package GPAW [17]. Additionally, we simulate the transmission using *ab initio* molecular dynamics within the Born–Oppenheimer approximation (BOMD) employing density functional theory (DFT) to calculate the forces [18–21]. In these simulations we use a 5×5 supercell of graphene, a computational grid spacing of 0.2 Å, a Monkhorst–Pack k-point mesh of $5 \times 5 \times 1$ [22], and timesteps of 1 as for TDDFT and 0.1 fs for BOMD. The PBE functional was used for all simulations [23]. From the simulations we obtain a barrier of 3.8 ± 1.3 eV for atomic hydrogen to penetrate graphene at the center of the hexagonal ring and a kinetic energy of 82.5 ± 2.5 eV for it to sputter a single carbon atom from the membrane in a head-on collision. These two energy values define a window for an H atom to penetrate graphene without inducing defects.

2.1. Proposed experimental setup

Neither supersonic nor hyperthermal atomic sources can reach a beam velocity of $v_z \geqslant 27\,000$ m s^{-1} needed to overcome the barrier of 3.8 eV. However, intense proton beams with a minimum energy of 5 eV, an energy resolution ΔE close to 1 eV and high directionality can be created using commercial ion guns. The required neutralization can be achieved, for instance, by using a 10–30 mm long neutralization cell filled with O_2 [24–26]. The proposed setup is sketched in figure 1. An ion gun is used to prepare a beam of H^+ with an energy between 5 and 80 eV. The protons are neutralized by resonant charge transfer in an effusive gas cell filled with molecular oxygen and remaining ions are deflected by a static electric field. The neutral H beam is collimated with two circular apertures of width s_1 and s_2 that limit the angular divergence to $\Delta\varphi = (s_1 + s_2)/2L_1 = 200$ μrad. At the grating the atoms are diffracted according to their de Broglie wavelength $\lambda_{dB} = h/m_H v_z$ with Planck's constant h and the mass of atomic hydrogen m_H. The wavelength lies between 14.7 and 3.2 pm for the 3.8−80 eV energy window, comparable to the wavelengths used in molecular matter-wave diffraction experiments [27, 28]. For H at a kinetic energy of 80 eV and $s_1 = 200$ μm, the transverse coherence amounts to $\ell_T = 2\,L_1 h/(s_1 m_H v_z) = 32$ nm. While this covers not even two slits of state-of-the-art nanomechanical gratings [29], it is sufficient to coherently illuminate several thousand hexagons of the graphene membrane. The diffraction pattern can be recorded in the optical far-field, i.e. the Fraunhofer regime at a distance L_2 behind the grating by a micro-channel plate stacked onto a phosphor screen. The expected atomic count rate at the detector increases with velocity, reaching $\approx 5 \times 10^4$ atoms s^{-1} at the border of the sputter region (supplementary material available online at stacks.iop.org/NJP/21/033004/mmedia). In the following we will discuss the case of atoms traveling at 80 eV, i.e. with an energy just below the knock-out threshold, to maximize the total transmission.

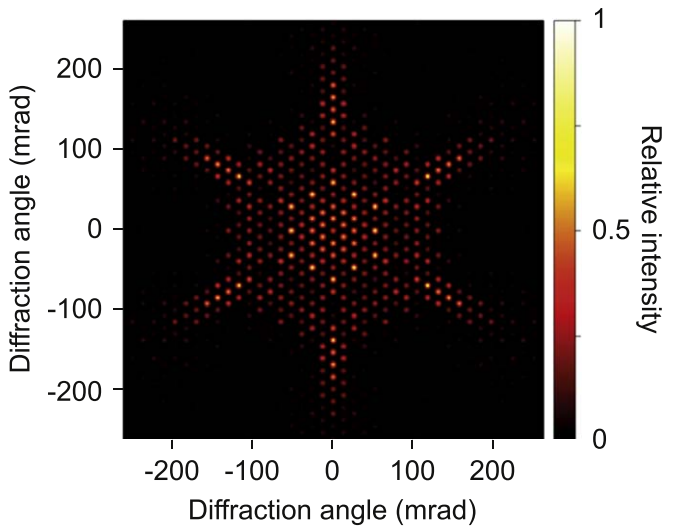

Figure 2. Intensity of the diffraction peaks as a function of the transferred in-plane momentum at $E_{\mathrm{kin}} = 80$ eV. For $L_1 = 1$ m the shown region corresponds to 58×58 cm^2.

3. Graphene-H interaction

The interaction of atomic hydrogen with graphite and graphene has been studied extensively over decades [30]. This is motivated by processes occurring in fusion reactors [31], possible routes leading to the formation of molecular hydrogen in space [32], and approaches to manipulate the properties of graphene [33, 34]. The predicted physisorption binding energy of hydrogen atoms on graphene is on the order of 40 meV [35], and depends critically on the level of theory and the correction of basis set superposition errors [36]. In the present study we describe the interaction of H with graphene using the PBE functional. Neglecting van der Waals (vdW) interactions in this approach is justified by the high kinetic energy of the hydrogen atoms of 80 eV, which is three orders of magnitude higher than the respective vdW binding energy. However, for low kinetic energies down to 5 eV these effects may have a strong influence and more elaborate approaches are likely needed.

To compute the atomic diffraction pattern behind single-layer graphene, the potential V between graphene and a hydrogen atom is required over the whole space region. Here, we assume that $V(x, y, z)$ is proportional to the electrostatic potential ρ_0 of graphene with an atom-specific scaling factor α [37]

$$V(x, y, z) = \alpha \rho_0(x, y, z), \tag{1}$$

where $\rho_0(x, y, z)$ is derived from the all-electron density [38]. We find the scaling factor $\alpha = -0.73$ by comparing the projected electrostatic potential $\rho_0(x, y) = \int \rho_0(x, y, z)\mathrm{d}z$ with the projected explicit DFT potential for a transmission through the center of the hexagon (supplementary material).

Based on the interaction potential we describe the diffraction process using two different methods. In the full quantum wave-packet calculation [39] the atomic matter-wave is diffracted at the 3D potential, while in the eikonal approximation only the projected potential along the z-direction $V(x, y)$ is used. At $E_{\mathrm{kin}} = 80$ eV the diffraction pattern obtained within the eikonal approximation reproduces the WPP calculations well, confirmed by a correlation of 94%. This demonstrates that the computationally less demanding eikonal approximation is a valid approach at this energy (supplementary material). The atomic diffraction pattern shown in figure 2 mirrors the hexagonal symmetry of graphene. For $L_2 = 1$ m and $E_{\mathrm{kin}} = 80$ eV the region displayed corresponds to 58×58 cm^2 in real space.

4. Coupling of the matter-wave to the membrane

This simulation shown in figure 2 is based on the assumption that the coherence of the matter-wave is conserved during diffraction. However, in transmission through the graphene membrane, the hydrogen atom is always closer than 142 pm to a carbon atom and their interaction might lead to decoherence of the matter-wave. Pictorially speaking, interference fringe visibility is lost when the de Broglie wavelength associated with the collisional momentum transfer $\lambda = \Delta p/h$ is shorter than twice the separation of two hexagons [40–42]. To describe the interaction between the diffracted atom and the membrane, we have simulated the transmission of H atoms in normal incidence at different positions in the hexagon. This allows us to quantify its coupling to the

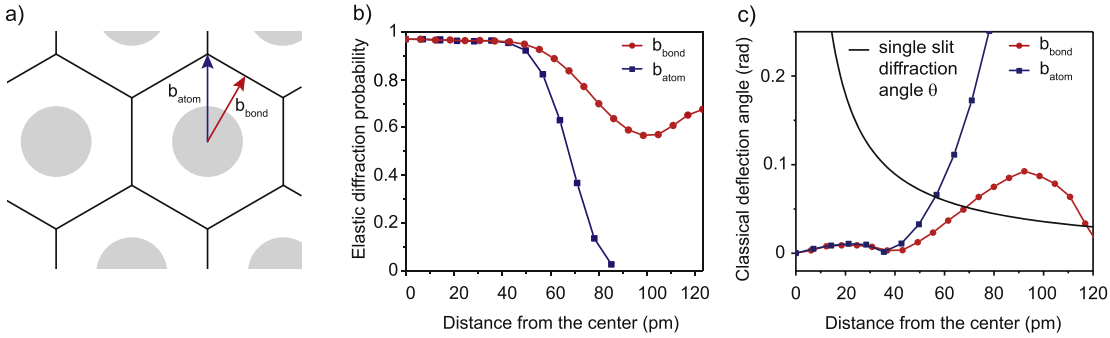

Figure 3. (a) Definition of the impact parameters b_{atom} and b_{bond}. The distance from the center of the hexagon to the atom (middle of the bond) amounts to 142 pm (123 pm). Transmission through the grey-shaded disc of about 110 pm diameter is expected to be mainly coherent as described by the Debye–Waller factor (DWF). (b) The probability for coherent diffraction according to the DWF (equation (3)) as a function of distance from the center of the hexagon. (c) Deflection angle of the H atoms for b_{atom} and b_{bond} and the single-slit diffraction angle θ associated with the second minimum of the Airy disc (full black line). At 80 eV only atoms transmitted through the central disc ($r \leqslant 60$ pm) are scattered at an angle smaller than ≈60 mrad.

electronic and nuclear degrees of freedom of the membrane. Starting from the center of the hexagon, the point of impact is varied towards a carbon atom (b_{atom}) and towards a C–C bond (b_{bond}) (figure 3(a)).

4.1. Coupling to the electronic system of graphene

For central transmission of the H atom, the BOMD simulations predict an energy loss of $\Delta E_{\mathrm{kin}} = 0.09$ eV. When the electronic degrees of freedom are taken into account (TDDFT), this value increases to 3.5 eV. The momenta of the carbon atoms are comparable in both simulations (supplementary material), indicating that the difference in energy is transferred to the electronic system of graphene. The energetically lowest in-plane plasmon in graphene has an energy around 4.7 eV and a wavelength on the order of $\lambda_{\mathrm{plas}} \approx 7$ nm [43, 44]. Excitation of such a plasmon can localize the H atom to $\lambda_{\mathrm{plas}}/2 \approx 3.5$ nm. As the resulting area encompasses still more than 100 hexagons, this effect will only lead to partial decoherence of the matter-wave. For impact parameters closer to the C atom/C–C-bond, the energy transfer increases slightly to 4.5 eV, resulting in a comparable localization. While the coherence of the matter-wave is reduced by inelastic scattering, the period of the graphene lattice is so small that even plasmonic excitations are still compatible with a high degree of coherence of the transmitted atomic wave function.

4.2. Coupling to the nuclear motion

Coupling to nuclear motion could also lead to (partial) decoherence of the transmitted matter-wave. To elucidate whether this is the case for the momentum transfer Δp_{coll} from the H atom to the C atoms, we compare the respective BOMD value to the intrinsic momentum uncertainty p_{uncert} of carbon atoms in graphene. If $\Delta p_{\mathrm{coll}} < p_{\mathrm{uncert}}$, it is fundamentally impossible for the membrane to resolve the position of the diffracted particles and atomic coherence should be maintained. We estimate p_{uncert} using the in-plane and out-of-plane mean square velocities $\langle v^2 \rangle$ [45] and the mass m_{C} of the carbon atoms

$$p_{\mathrm{uncert}} = \sqrt{\langle v^2 \rangle} \times m_{\mathrm{C}}. \tag{2}$$

At the zero-point vibrational level this yields an average out-of-plane momentum of $p_{\perp} \cong 1.0 \times 10^{-23}$ kg m s^{-1} and an in-plane momentum of $p_{\parallel} \cong 2.1 \times 10^{-23}$ kg m s^{-1}. The mean square velocities $\langle v^2 \rangle$ have been calculated *ab initio* within the harmonic approximation and the equipartition of thermal energy based on the phonon density of states [45].

The simulation, as well as momentum conservation, suggest that the H atom couples primarily to the in-plane motion of the C atoms. We therefore use $p_{\parallel}$ as a good measure for the onset of decoherence. Let us assume that the overall momentum change of the hydrogen atom $\Delta p(\mathrm{H}) = |p(\mathrm{H})_{\mathrm{initial}} - p(\mathrm{H})_{\mathrm{final}}|$ is equally distributed over only the nearest six C atoms at central transmission. While this is non-physical, as this hexagon is not isolated from the rest of the membrane, it represents a hypothetical worst-case scenario. Even in this case, we expect a momentum transfer of 3×10^{-24} kg m s^{-1} per C atom, well below the momentum uncertainty. This applies also to the instantaneous momentum transfer (supplementary material) and suggests that coupling to the nuclear motion is compatible with coherent diffraction.

In an actual experiment, decoherence is a gradual process in which the hydrogen atom couples more and more to the phonons and plasmons of the lattice. The probability of elastic diffraction can be estimated assuming that the C atoms behave like independent harmonic oscillators and the energy transfer between H and

graphene is fast through a single C–H interaction. After a momentum transfer of Δp, the wave function of the C atom $\chi(R)$ becomes $e^{-i\Delta pR/\hbar}\chi(R)$ [46]. For a 1D harmonic oscillator the elastic diffraction probability P_e is then described by the Debye–Waller factor (DWF) [47]

$$\mathrm{DWF} \equiv P_e = |\langle\chi|\exp(i\Delta pR/\hbar)|\chi\rangle|^2 = \exp\left(-\frac{\Delta p^2\langle R^2\rangle}{2\hbar^2}\right). \quad (3)$$

Using the aforementioned *ab initio* calculations, we extract an in-plane mean-squared displacement $\langle R^2\rangle$ at 0 K of 15.3 pm^2 [48, 49]. The resulting position-dependent probability of coherent transmission along b_{atom} and b_{bond} is shown in figure 3(b). At the center of the hexagon P_e amounts to 97% and remains above 80% for distances from the center of less than 57 (b_{atom}) and 70 pm (b_{bond}). For larger distances P_e drops, reaching zero at ≈80 pm (b_{atom}). However, for a trajectory this close to a carbon atom, the H atom is classically deflected by an angle larger than the maximum diffraction angle. If we approximate the open area of a hexagon as a circle with diameter D, its single-slit diffraction pattern is described by an Airy disc and the second minimum is at an angle $\theta = 7.02\lambda_{\mathrm{dB}}/\pi D$. The H atom is deflected beyond this region for $D \geqslant 110$ (b_{atom}) and 140 pm (b_{bond}) as shown in figure 3(c). Inside these circles the probability for elastic diffraction is still above 80%. This indicates that coherent transmission is likely through roughly a sixth of the area of graphene (grey-shaded areas in figure 3(a)). It also shows that most of the inelastically diffracted atoms are deflected to larger angles and thus spatially well separated from the coherent diffraction signal.

4.3. Realistic diffraction pattern

In this proposal we consider that each atom is diffracted at a membrane in thermal equilibrium. This is reasonable as phonons excited by the H atoms are damped on the ps time scale [45], much shorter than the expected arrival rate of individual atoms at the grating, which is on the order of one hydrogen atom per hexagon and second. In a realistic diffraction pattern, the observed contrast is reduced due to a number of effects. These are thermal vibrations, the finite transverse and longitudinal coherence of the diffracted beam, and inelastic effects related to both electronic and phononic excitations of graphene. The effect of phonons is accounted for by computing the diffraction pattern obtained from a rigid but distorted graphene sheet where the C atoms are randomly shifted from their equilibrium position in such a way that $\langle R^2\rangle$ reproduces the extension of the vibrational wave function at 300 K. In contrast to phononic excitations, electronic excitations are associated with a very small momentum transfer, because of the mass difference between an electron and an H atom. The effect of electronic excitation is then an increase in the energy dispersion of the atomic beam. In principle also the finite coherence length of a polycrystalline graphene sheet has be taken into account. However, recent progress has led to millimeter-sized single crystals of graphene [50, 51]. Hence, we consider only diffraction at a perfect crystal in a single orientation.

The resulting realistic diffraction pattern is shown in figure 4. It is obtained from a sample of graphene of 256 elementary cells (i.e. 3.7 × 3.7 nm^2). Both in-plane and out-of-plane displacements of the C atoms have been considered, although the latter ones have no significant effect. The observed incoherent background is due to excitations of phonons in the membrane. While corrugations of the membrane would lead to an additional smearing of the diffraction orders as observed in electron microscopy [52], these can be reduced by strain-engineering the membrane [53, 54], and are not considered here. The angular resolution has been taken to be $\delta\varphi = 200\ \mu$rad (FWHM), the initial energy resolution of the H beam is $\Delta E/E = 1\%$, and coupling to the electronic system of graphene is accounted for by an additional broading of $\Delta E/E = 5\%$. We predict a signal-to-background ratio between 30 and 140 for diffraction angles up to 52 mrad.

5. Discussion

Our simulations indicate that the atoms get only weakly localized during transmission even though they interact with the electronic and nuclear degrees of freedom of graphene. While the wavelength of the considered atom is comparable to current studies in molecular matter-wave diffraction, the period d of the grating is more than 400 times smaller, leading to widely separated diffraction orders. The maximum considered diffraction angle of 52 mrad corresponds to a transverse velocity uncertainty of ±6400 m s^{-1} for hydrogen. To acquire a comparable momentum kick h/d in a laser grating, a cesium atom would have to accumulate 13850 $\hbar k_{\mathrm{Cs}}$, expressed in multiples of k_{Cs} for $\lambda_{\mathrm{Cs}} = 2\pi/k_{\mathrm{Cs}} = 852$ nm. While comparable diffraction angles can be reached with fast atoms at LiF(001) surfaces [25, 55], where up to 50% elastic diffraction has been observed, the graphene transmission beam splitter is much more compact.

As an alternative, we also considered the diffraction of helium. According to our simulations, the window of energies which can be used for defect-free transmission lies between 13.5 ± 0.5 and 37.5 ± 2.5 eV. However, helium is considerably larger than a hydrogen atom, leading to stronger couplings to nuclear motion. For central transmission, we predict an in-plane momentum transfer to the closest carbon atoms of 0.9 × 10^{-23} kg m s^{-1},

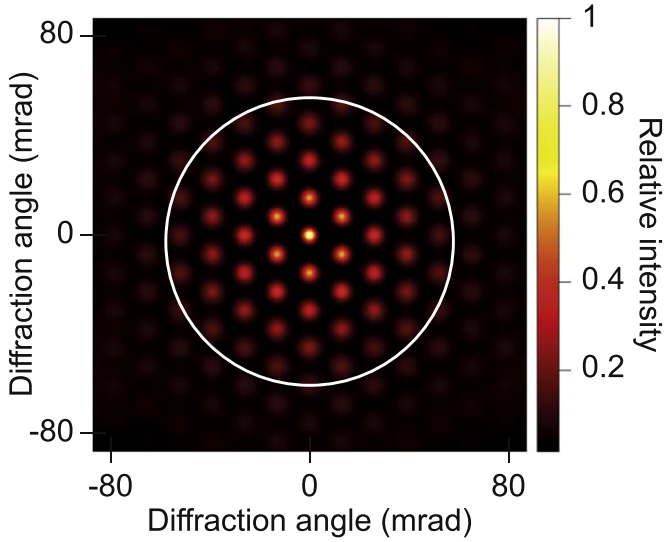

Figure 4. Diffraction pattern including the discussed decoherence effects. Around 8% of the atoms are diffracted by less than 52 mrad (white circle). The predicted signal-to-background ratio reaches up to 140.

which is only a factor of two smaller than the in-plane momentum uncertainty of $p_{\parallel} \cong 2.1 \times 10^{-23}$ kg m s^{-1}. Furthermore, the energy loss of the He atom amounts to about 1.5 eV which couples almost entirely to the nuclear motion. Hence, the respective DWF amounts to only 28% even at the center, suggesting a considerably worse signal to noise ratio for helium than for hydrogen. In combination with atomic hydrogen also the diffraction through other mono-layered membranes such as hexagonal boron nitride seems possible. While it is likely that the kinetic energy of the diffracted atom has to be adapted to comply with the reduced mechanical stability compared to single-layer graphene, studying these differences might be important for modifying 2D membranes with fast atoms.

The large diffraction angle of H at graphene makes it an interesting element for Mach–Zehnder interferometers with very large enclosed areas. The required stability of the setup is comparable to neutron interferometry [56]. The natural corrugation of graphene [52] may be an issue, but can be reduced by straining the lattice and it has only a minor influence in single-grating Fraunhofer diffraction [57, 58]. The proposed setup could be used, for instance, to conduct comparative measurements on hydrogen and deuterium, a pair that is expected to be particularly sensitive to tests of the Einstein equivalence principle [59]. For such an experiment, H and D could be prepared by two individual ion guns, producing matter-waves with the same de Broglie wavelength despite their difference in mass. Sending the atoms through the same apertures s_1 and s_2 ensures identical paths of the two species through the interferometer.

Note that the disintegration of graphite has been observed under bombardment with hydrogen and deuterium ions [60]. However, this process is described as the interplay between adsorption and intercalation which leads to the removal and subsequent fragmentation of graphite layer by layer [61, 62]. In our setting this etching pathway is excluded as intercalation is not possible. In turn, this restricts the proposed method to single-layered materials. Also physisorption and chemisorption of hydrogen atoms on the membrane does not necessarily limit the performance of the grating. While especially the latter leads to profound changes in the mechanical stability of graphene [63], adsorbed hydrogen atoms can be effectively removed by keeping the membrane at elevated temperatures [64, 65].

6. Conclusion

We have shown that atomic hydrogen at a kinetic energy of 80 eV has a high probability to be coherently transmitted through about a sixth of the area of graphene. While molecular dynamics simulations based on time-dependent density functional theory reveal pronounced couplings of the matter-wave to both the nuclear and the electronic degrees of freedom, these interactions are compatible with coherent diffraction. The combination of graphene with fast atomic hydrogen can thus become the basis for both very small and extremely large matter-wave interferometers. In near-field matter-wave interferometry, the natural grating separation is the Talbot-distance $d^2/\lambda_{\mathrm{dB}}$ which amounts to 19 nm at 80 eV energy. This would allow building a closed atom interferometer on the sub-μm scale. On the other hand, the mean free path of an H atom can easily reach the km-range at high vacuum. While the atom spends only 8 ms in a 1 km long interferometer, the maximum spatial

separation of the diffraction orders is on the order of 50 m. This may provide a valuable platform for precision tests of quantum mechanics [66, 67]. It may also be a promising basis for gravitational wave detectors based on matter-wave interferometry [68, 69] as the sensitivity is determined by the kinetic energy of the interfering particle [70, 71], which is here more than 10^8 times larger than in cold atom interferometry experiments.

Acknowledgments

This project has received funding from the European Research Council (ERC) under the European Union's Horizon 2020 research and innovation programme (grant agreement no. 320694) and from the Austrian Science Fund FWF (P-30176, P28322-N36, and P31605). We thank Professor E E Campbell and Dennis Schlippert for fruitful discussions and the Vienna Scientific Cluster for computational resources.

ORCID iDs

Christian Brand https://orcid.org/0000-0003-3872-7769
Toma Susi https://orcid.org/bp0000-0003-2513-573X
Jani Kotakoski https://orcid.org/0000-0002-1301-5266
Philippe Roncin https://orcid.org/0000-0002-7407-9474
Markus Arndt https://orcid.org/0000-0002-9487-4985

References

[1] de Broglie L 1923 *Nature* **112** 540
[2] Davisson C and Germer L H 1927 *Nature* **119** 558–60
[3] Thomson G P 1927 *Nature* **120** 802–802
[4] von Halbon H and Preiswerk P 1936 *C. R. Acad. Sci., Paris* **203** 73–5
[5] Estermann I and Stern O 1930 *Z. Phys.* **61** 95–125
[6] Johnson T H 1930 *Phys. Rev.* **35** 1299–300
[7] Miao M, Nardelli M B, Wang Q and Liu Y 2013 *Phys. Chem. Chem. Phys.* **15** 16132–7
[8] Leenaerts O, Partoens B and Peeters F M 2008 *Appl. Phys. Lett.* **93** 193107
[9] Bunch J S, Verbridge S S, Alden J S, van der Zande A M, Parpia J M, Craighead H G and McEuen P L 2008 *Nano Lett.* **8** 2458–62
[10] Campbell E E B, Ehlich R, Heusler G, Knospe O and Sprang H 1998 *Chem. Phys.* **239** 299–308
[11] Walter M, Häkkinen H, Lehtovaara L, Puska M, Enkovaara J, Rostgaard C and Mortensen J J 2008 *J. Chem. Phys.* **128** 244101
[12] Runge E and Gross E K U 1984 *Phys. Rev. Lett.* **52** 997–1000
[13] Leeuwen R V 2001 *Int. J. Mod. Phys.* B **15** 1969–2023
[14] Vignale G 2008 *Phys. Rev.* A **77** 062511
[15] Ruggenthaler M and Leeuwen R V 2011 *Europhys. Lett.* **95** 13001
[16] Ojanperä A, Krasheninnikov A V and Puska M 2014 *Phys. Rev.* B **89** 035120
[17] Enkovaara J *et al* 2010 *J. Phys.: Condens. Matter* **22** 253202
[18] Hohenberg P and Kohn W 1964 *Phys. Rev.* **136** B864–71
[19] Kohn W and Sham L J 1965 *Phys. Rev.* **140** A1133–8
[20] Lammert P E 2007 *Int. J. Quantum Chem.* **107** 1943–53
[21] Lieb E H 1983 *Int. J. Quantum Chem.* **24** 243–77
[22] Monkhorst H J and Pack J D 1976 *Phys. Rev.* B **13** 5188–92
[23] Perdew J P, Burke K and Ernzerhof M 1996 *Phys. Rev. Lett.* **77** 3865–8
[24] Rousseau P, Khemliche H, Borisov A G and Roncin P 2007 *Phys. Rev. Lett.* **98** 016104
[25] Schüller A, Wethekam S and Winter H 2007 *Phys. Rev. Lett.* **98** 016103
[26] Gao R S, Johnson L K, Hakes C L, Smith K A and Stebbings R F 1990 *Phys. Rev.* A **41** 5929–33
[27] Arndt M, Nairz O, Vos-Andreae J, Keller C, van der Zouw G and Zeilinger A 1999 *Nature* **401** 680–2
[28] Brand C, Eibenberger S, Sezer U and Arndt M 2016 Matter-wave physics with nanoparticles and biomolecules *Les Houches Summer School, Session CVII—Current Trends in Atomic Physics* (Oxford: Oxford University Press)
[29] Brand C *et al* 2015 *Nat. Nanotechnol.* **10** 845–8
[30] Bonfanti M, Achilli S and Martinazzo R 2018 *J. Phys.: Condens. Matter* **30** 283002
[31] Roth J and Garcia-Rosales C 1997 *Nucl. Fusion* **36** 1647–59
[32] Tielens A G G M 2013 *Rev. Mod. Phys.* **85** 1021–81
[33] Boukhvalov D W, Katsnelson M I and Lichtenstein A I 2008 *Phys. Rev.* B **77** 035427
[34] Balog R *et al* 2010 *Nat. Mater.* **9** 315–9
[35] Ghio E, Mattera L, Salvo C, Tommasini F and Valbusa U 1980 *J. Chem. Phys.* **73** 556–61
[36] Bonfanti M and Martinazzo R 2018 *Phys. Rev.* B **97** 117401
[37] Ehemann R C, Krstić P S, Dadras J, Kent P R and Jakowski J 2012 *Nanoscale Res. Lett.* **7** 198
[38] Susi T, Madsen J, Ludaka U, Mortensen J J, Pennycook T J, Lee Z, Kotakoski J, Kaiser U and Meyer J C 2019 *Ultramicroscopy* **197** 16–22
[39] Broeckhove J and Lathouwers L (ed) 1992 *Time-Dependent Quantum Molecular Dynamics* (*NATO ASI Series*) (New York: Plenum)
[40] Chapman M S, Hammond T D, Lenef A, Schmiedmayer J, Rubenstein R A, Smith E and Pritchard D E 1995 *Phys. Rev. Lett.* **75** 3783–7
[41] Kokorowski D A, Cronin A D, Roberts T D and Pritchard D E 2001 *Phys. Rev. Lett.* **86** 2191–5
[42] Pfau T, Spälter S, Kurtsiefer C, Ekstrom C R and Mlynek J 1994 *Phys. Rev. Lett.* **73** 1223–6
[43] Eberlein T, Bangert U, Nair R R, Jones R, Gass M, Bleloch A L, Novoselov K S, Geim A and Briddon P R 2008 *Phys. Rev.* B **77** 233406
[44] Egerton R F 2017 *Ultramicroscopy* **180** 115–24

[45] Susi T, Hofer C, Argentero G, Leuthner G T, Pennycook T J, Mangler C, Meyer J C and Kotakoski J 2016 *Nat. Commun.* **7** 13040
[46] Mössbauer R L and Sharp D H 1964 *Rev. Mod. Phys.* **36** 410–7
[47] Roncin P and Debiossac M 2017 *Phys. Rev.* B **96** 035415
[48] Allen C S, Liberti E, Kim J S, Xu Q, Fan Y, He K, Robertson A W, Zandbergen H W, Warner J H and Kirkland A I 2015 *J. Appl. Phys.* **118** 074302
[49] Susi T and Kotakoski J 2016 *J. Appl. Phys.* **119** 066101
[50] Gao L *et al* 2012 *Nat. Commun.* **3** 699
[51] Nguyen V L and Lee Y H 2015 *Small* **11** 3512–28
[52] Meyer J C, Geim A K, Katsnelson M I, Novoselov K S, Booth T J and Roth S 2007 *Nature* **446** 60–3
[53] Nicholl R J T, Lavrik N V, Vlassiouk I, Srijanto B R and Bolotin K I 2017 *Phys. Rev. Lett.* **118** 266101
[54] Ludacka U, Monazam M R A, Rentenberger C, Friedrich M, Stefanelli U, Meyer J C and Kotakoski J 2018 *npj 2D Mater. Appl.* **2** 25
[55] Debiossac M, Zugarramurdi A, Lunca-Popa P, Momeni A, Khemliche H, Borisov A G and Roncin P 2014 *Phys. Rev. Lett.* **112** 023203
[56] Rauch H and Werner S 2000 *Neutron Interferometry: Lessons in Experimental Quantum Mechanics* (*Oxford Series of Neutron Scattering on Condensed Matter* vol 12) (Oxford: Oxford University Press)
[57] Keith D W, Ekstrom C R, Turchette Q A and Pritchard D E 1991 *Phys. Rev. Lett.* **66** 2693–6
[58] Perreault J D and Cronin A D 2005 *Phys. Rev. Lett.* **95** 133201
[59] Hohensee M A and Müller H 2011 *J. Mod. Opt.* **58** 2021–7
[60] Roth J and Bohdansky J 1987 *Nucl. Instrum. Methods Phys. Res.* B **23** 549–51
[61] Nakamura H and Ito A 2007 *Mol. Simul.* **33** 121–6
[62] Ito A and Nakamura H 2008 *Commun. Comput. Phys.* **4** 592–610
[63] Pei Q X, Zhang Y W and Shenoy V B 2010 *Carbon* **48** 898–904
[64] Hornekær L, Rauls E, Xu W, Šljivančanin Ž, Otero R, Stensgaard I, Lægsgaard E, Hammer B and Besenbacher F 2006 *Phys. Rev. Lett.* **97** 186102
[65] Wojtaszek M, Tombros N, Caretta A, van Loosdrecht P H M and van Wees B J 2011 *J. Appl. Phys.* **110** 063715
[66] Zych M, Costa F, Pikovski I and Brukner C 2011 *Nat. Commun.* **2** 505
[67] Diósi L 1987 *Phys. Lett.* A **120** 377–81
[68] Chiao R Y and Speliotopoulos A D 2004 *J. Mod. Opt.* **51** 861–99
[69] Graham P W, Hogan J M, Kasevich M A and Rajendran S 2013 *Phys. Rev. Lett.* **110** 171102
[70] Lamine B, Hervé R, Lambrecht A and Reynaud S 2006 *Phys. Rev. Lett.* **96** 050405
[71] Roura A, Brill D R, Hu B L, Misner C W and Phillips W D 2006 *Phys. Rev.* D **73** 084018